Received: 27 December 2016 | Revised: 10 May 2017 | Accepted: 10 May 2017

DOI: 10.1002/jnr.24096

RESEARCH ARTICLE

WILEY

mfat-1 transgene protects cultured adult neural stem cells against cobalt chloride–mediated hypoxic injury by activating *Nrf2/ARE* pathways

Junfeng Yu[1†] | Haiyuan Yang[1†] | Bin Fang[1] | Zhengwei Zhang[2] | Ying Wang[1] | Yifan Dai[1]

[1]Jiangsu Key Laboratory of Xenotransplantation, Nanjing Medical University, Nanjing, People's Republic of China

[2]Huaian First Hospital Affiliated to Nanjing Medical University, Huai'an, People's Republic of China

Correspondence
Dr. Yifan Dai and Dr. Ying Wang. Jiangsu Key Laboratory of Xenotransplantation, Nanjing Medical University, 101 Longmian Avenue, Nanjing, 211166, People's Republic of China. Phone: 0086-25-86869477.
Email: daiyifan@njmu.edu.cn and ywang@njmu.edu.cn.

Funding information
This work was supported by the National Natural Science Foundation of China (no. 81570402) and the Sanming Project of Medicine in Shenzhen, Fund for High Level Medical Discipline Construction of Shenzhen (no. 2016031638); Yifan Dai, Ying Wang, and Haiyuan Yang are Fellows at the Collaborative Innovation Center for Cardiovascular Disease Translational Medicine, Nanjing Medical University.

Abstract

Ischemic stroke is a devastating neurological disorder and one of the leading causes of death and serious disability in adults. Adult neural stem cell (NSC) replacement therapy is a promising treatment for both structural and functional neurological recovery. However, for the treatment to work, adult NSCs must be protected against hypoxic-ischemic damage in the ischemic penumbra. In the present study, we aimed to investigate the neuroprotective effects of the mfat-1 transgene on cobalt chloride ($CoCl_2$)-induced hypoxic-ischemic injury in cultured adult NSCs as well as its underlying mechanisms. The results show that in the $CoCl_2$-induced hypoxic-ischemic injury model, the *mfat-1* transgene enhanced the viability of adult NSCs and suppressed $CoCl_2$-mediated apoptosis of adult NSCs. Additionally, the mfat-1 transgene promoted the proliferation of NSCs as shown by increased bromodeoxyuridine labeling of adult NSCs. This process was related to the reduction of reactive oxygen species. Quantitative real-time polymerase chain reaction and Western blot analysis revealed a much higher expression of nuclear factor erythroid 2-related factor 2 (*Nrf2*) and its downstream genes (*HO-1*, *NQO-1*, *GCLC*). Taken together, our findings show that the mfat-1 transgene restored the $CoCl_2$-inhibited viability and proliferation of NSCs by activating nuclear factor erythroid 2-related factor 2 (*Nrf2*)/antioxidant response elements (*ARE*) signal pathway to inhibit oxidative stress injury. Further investigation of the function of the mfat-1 transgene in adult protective mechanisms may accelerate the development of adult NSC replacement therapy for ischemic stroke.

KEYWORDS

mfat-1 gene, adult neural stem cells (NSCs), ischemic stroke, cobalt chloride ($CoCl_2$), oxidative stress, nuclear factor erythroid 2-related factor 2 (*Nrf2*), RRID: IMSR_-JAX:000664, RRID: AB_1645170, RRID: AB_94872, RRID: AB_2109645, RRID: AB_570918, RRID: AB_302944, RRID: AB_944418, RRID: AB_11156457, RRID: AB_881738, RRID: AB_2107804, RRID: AB_2107436, RRID: AB_306966, RRID: SCR_003070, RRID: SCR_007369, RRID: SCR_002865

1 | INTRODUCTION

Ischemic stroke, also known as cerebrovascular accident, is one of the leading causes of death and serious long-term disability in adults across the world (Mozaffarian et al., 2016). There is currently no therapy that sufficiently improves clinical recovery after ischemic stroke (Sims & Muyderman, 2010; Stankowski & Gupta, 2011). Adult neural stem cell (NSC) replacement therapy is a promising treatment for neurological recovery both structurally and functionally: It includes endogenous NSC regeneration to replace damaged tissue or neural cells in adulthood and exogenous adult NSC transplant after injuries such as ischemic stroke (Arvidsson, Collin, Kirik, Kokaia, & Lindvall, 2002; Chung et al., 2015; Koch, Kokaia, Lindvall, & Brustle, 2009; Paradisi et al., 2014). Adult NSCs are clinically important not only because ischemic

[†]Junfeng Yu and Haiyuan Yang contributed equally to this work.

Significance

Adult neural stem cell (NSC) replacement therapy has become a promising treatment for ischemic stroke in recent years. The primary obstacle is that hypoxic-ischemic damage inhibits the activity of adult NSCs and impairs their physiological function. In this study, an mfat-1 transgene mouse model was used to investigate whether overproduction of omega-3 polyunsaturated fatty acids could protect adult NSCs against hypoxic damage induced by cobalt chloride ($CoCl_2$). Our results demonstrate for the first time that mfat-1 protects adult NSCs against $CoCl_2$-mediated hypoxic injury by activating nuclear factor erythroid 2-related factor 2/antioxidant response pathways. These results are important for innovating clinical intervention strategies for ischemic stroke.

stroke occurs mainly in adults but also because they are easy to obtain, with no medical ethics problems and no tumorigenicity (Giusto, Donega, Cossetti, & Pluchino, 2014). In the ideal scenario, soon after ischemic stroke, endogenous or exogenous adult NSCs would exhibit proliferation, migration, and differentiation to repair neural function damage (Chung et al., 2015; Cramer, 2008). However, because of the loss of nutrients and oxygen in the ischemic penumbra, the majority of newly generated NSCs die soon after stroke, and their physiological function is lost (Azevedo-Pereira & Daadi, 2013; Bazan, Marcheselli, & Cole-Edwards, 2005; Rosenblum et al., 2015). Therefore, figuring out how to protect adult NSCs against hypoxic-ischemic injury after ischemic stroke is key to effective adult NSC replacement therapy.

Omega-3 polyunsaturated fatty acids (n-3 PUFAs) have sparked clinical interest in their therapeutic application for promoting the survival, migration, proliferation, and differentiation of adult NSCs during replacement therapy in ischemic stroke. n-3 PUFAs are essential for human beings, helping to maintain cellular membrane structural and functional integrity (Antonny, Vanni, Shindou, & Ferreira, 2015). Moreover, PUFAs are highly enriched in the brain and play a key role in brain development and repair under many conditions (Chang et al., 2012). Decades of research have provided insight into the elevation of the n-3/n-6 PUFA ratio, demonstrating that a higher ratio rather than n-3 PUFAs exerts beneficial effects in a variety of neurological disorders, including ischemic stroke (Belayev, Khoutorova, Atkins, & Bazan, 2009; Belayev et al., 2011; Hong, Belayev, Khoutorova, Obenaus, & Bazan, 2014; Hu et al., 2013; Liu et al., 2016; Zhang et al., 2010).

In this study, NSCs were cultured from an mfat-1 transgene mouse model that converts n-6 PUFAs to n-3 PUFAs in vivo, resulting in abundant endogenous n-3 PUFA, without changing total PUFA in their organs and tissue, through overexpressing the *C. elegans* n-3 fatty acid desaturase gene, mfat-1 (Wei et al., 2010). This mfat-1 transgene mouse model was firstly used to investigate whether overproduction of n-3 PUFAs could protect adult NSCs against hypoxic damage induced by cobalt chloride ($CoCl_2$), which is a well-known hypoxia-mimetic agent. There are numerous reports that $CoCl_2$ is widely used to mimic the hypoxic-ischemic microenvironment in various cultured cells (Chen, Zhao, & Huang, 2009; Lan et al., 2012; Sandner et al., 1997; Tan et al., 2009; Zou et al., 2001). Therefore, we used $CoCl_2$-treated adult NSCs as an in vitro model to study the adult NSCs' response to hypoxic-ischemic injury. And we demonstrated that elevation of the n-3/n-6 PUFAs ratio significantly enhanced the survival of adult NSCs in a $CoCl_2$-mediated hypoxic injury model, but the underlying molecular protective mechanisms are still not fully understood. It has been reported that oxidative stress–induced neuronal apoptosis plays an important role in the pathogenesis of ischemic stroke (Chehaibi, Trabelsi, Mahdouani, & Slimane, 2016; Yamauchi et al., 2016). Brain tissues and cells are rich in PUFAs, which are more susceptible to oxidative stress injury (Guichardant et al., 2004). Cellular defense against oxidative stress injury is mainly mediated by antioxidative enzymes and detoxifying enzymes, including glutathione (GSH), heme-oxygenase-1 (*HO-1*), glutamate cysteine ligase catalytic subunit (*GCLC*), and NADPH quinone oxidoreductase 1 (*NQO-1*) (Dinkova-Kostova & Talalay, 2008; Zhang et al., 2013). The expression of antioxidative enzymes and detoxifying enzymes is regulated by nuclear factor erythroid 2-related factor 2 (*Nrf2*), a transcription factor that plays a key role in cytoprotection against oxidative stress. Under normal conditions, Nrf2 is silenced by combining Kelch-like ECH-associated protein 1 (*Keap1*) (Kobayashi et al., 2004). *Keap1* is a cysteine-rich cytosolic protein that functions as an adaptor, leading to proteasomal degeneration of *Nrf2* via ubiquitination. Under stressful conditions, Nrf2-Keap-1 complexes are dissociated and *Nrf2* rapidly undergoes nuclear translocation, initiating the expression of antioxidative and detoxifying enzymes. Our investigation showed that the *Nrf2/ARE* signal pathway is involved in this process. The results are of great importance not only for broadening the theory on adult NSCs' protective mechanism after brain ischemic injury but also for innovating strategies for adult NSC clinical replacement therapy in ischemic stroke.

2 | MATERIALS AND METHODS

2.1 | Animals

In mfat-1 transgene mice, the coding region of *C. elegans fat-1* cDNA was optimized to enhance the expression of fat-1 in mammalian cells. The *mfat-1* cDNA driven by a cytomegalovirus enhancer and chicken β-actin promoter linked with a muscle creatine kinase enhancer was introduced into C57BL/6 mice (RRID: IMSR_-JAX:000664) by pronuclear microinjection (Wei et al., 2010). The mfat-1 heterozygotes of C57/B6 and wild-type (WT) C57/B6 mice were crossed to produce mfat-1 transgene mice and WT littermates. Both of them were bred in the Animal Core Facility of Nanjing Medical University. All animal experiments were approved by the Institutional Animal Care and Use Committee of Nanjing Medical University, China. Every effort was made to minimize animal suffering. All experiments were performed in accordance with the approved guidelines for animal care and management of research projects.

2.2 | Genomic DNA extraction and genotype identification

The adult (8–10 weeks) *mfat-1* transgenic mice and WT littermates were identified by genotyping using polymerase chain reaction (PCR) amplification. Genomic DNA was extracted from mice tails using a TIANamp Genomic DNA Kit (TIANGEN, Beijing, China). The PCR primers used for the *mfat-1* gene were forward 5′- GGACCTTGGTGAAGAG CATCCG-3′ and reverse 5′-GCGTCGCAGAAGCCAAAC-3′. PCR product was 438 bp. The PCR conditions were as follows: 94 °C for 5 min (1 cycle), 94 °C for 30 s, 65 °C for 30 s, and 72 °C for 60 s (35 cycles). The PCR products were separated by 1.5% agarose gel electrophoresis.

2.3 | Primary adult mouse NSCs isolation and culture

The primary adult NSCs were isolated from the subventricular zone (SVZ) of adult mfat-1 transgenic mice and WT littermates at 8 to 10 weeks. Briefly, NSCs from 8- to 10-week-old adult mfat-1 transgenic mice and adult WT littermates were designated as $NSCs^{fat\text{-}1}$ and $NSCs^{WT}$, respectively. First, under sterile conditions, the adult mouse brain was dissected out to a 60-mm tissue culture dish with cold phosphate buffer solution (PBS) (Gibco BRL, Grand Island, Ny, USA). Then, the coronal section of the brain was cut into 2- to 3-mm-thick slices with a new razor blade, and slices were placed in fresh PBS. The tissues were separated from SVZ with fine forceps under a dissecting microscope, then cut into small squares (approximately 1.0 mm^3) with forceps and put into 1.5-ml tubes containing SFM solution (described below). The tissues were then centrifuged for 5 min at 350*g*, followed by removal of the supernatant and lysing with 0.5 ml 1% trypsin (Gibco BRL, Grand Island, Ny, USA) at 37 °C for 20 min. After centrifuging for 5 min at 350*g*, the supernatant was removed, 0.5 ml of trypsin inhibitor was added (Roche, Mannheim, Germany), and the sample was centrifuged for 5 min at 350*g*. The cells were suspended in 0.5 ml of SFM and triturated sufficiently to produce a single-cell suspension. After adding 1.5 ml of SFM containing the cells to each well of a 12-well plate (Corning, Ny, USA), all cultures were incubated at 37 °C with 95% air and 5% CO_2.

The adult stem cells were floating-cultured in serum-free medium and passaged every 4 to 6 days when the neurospheres grew to a diameter of approximately 150 μm. The SFM consisted of DMEM/F12 medium (1:1; Gibco BRL, Grand Island, Ny, USA) containing 28.5 μmol/ml $NaHCO_3$ (Sigma-Aldrich, St. Louis, MO, USA) 33.3 μmol/ml glucose (Sigma-Aldrich, St. Louis, MO, USA), 1 nmol/ml HEPES buffer (Sigma-Aldrich, St. Louis, MO, USA), 0.2 nmol/ml progesterone (Sigma-Aldrich, St. Louis, MO, USA) 108.9 nmol/ml putrescine (Sigma-Aldrich, St. Louis, MO, USA), 2% B27 supplement (Molecular Probes; Invitrogen, Carlsbad, CA, USA), 1% insulin-transferrin-sodium selenite supplement (ITSS, Roche, Mannheim, Germany), 5 ng/ml basic fibroblast growth factor (FGF; Sigma-Aldrich, St. Louis, MO, USA), 20 ng/ml epidermal growth factor (EGF; Sigma-Aldrich, St. Louis, MO, USA), and 1.83 μg/ml heparin (Sigma-Aldrich, St. Louis, MO, USA). SFM was filtered with a 0.22-μm-pore-size filter after the addition of all components except the growth factors (FGF, EGF), B-27, and ITSS, which were added to the sterile SFM.

2.4 | Immunocytochemistry identification of $NSCs^{fat\text{-}1}$ and $NSCs^{WT}$

The primary neurospheres were passaged with Accutase solution (Sigma-Aldrich, St. Louis, MO, USA), and the passaged cells were called first passage (P1). The third passage cells were used for all the subsequent experiments. For immunocytochemistry identification experiments, the third passage cells were triturated to single cells and planted at a density of 1×10^5 cells per milliliter on dishes that were coated with Poly-D-Lysine (Sigma-Aldrich, St. Louis, MO, USA) and sterile laminin (Roche, Mannheim, Germany). For differentiation studies, EGF was omitted and FGF was used at half the concentration of SFM, and then 1% FBS was added (Gibco BRL, Grand Island, Ny, USA). The cultures were fully differentiated for up to 7 days.

For immunofluorescent staining, cells were fixed with 4% paraformaldehyde for 30 min and washed in PBS (Gibco BRL, Grand Island, Ny, USA), pH 7.4, for 10 min, 3 times. After blocking in PBS containing 5% goat serum and 0.3% Triton X-100 at room temperature for 1 hr, the cells were incubated with primary antibodies at 4 °C overnight. The primary antibodies used were as follows: mouse anti-nestin (BD Biosciences, 556309, RRID: AB_1645170), rabbit anti-NeuN (Abcam, ab177487, RRID: AB_2532109), chicken anti-β-III-tubulin (Millipore Bioscience Research Reagents, AB9354, RRID: AB_570918), mouse anti–glial fibrillary acidic protein (GFAP) (Millipore Bioscience Research Reagents, AB5804, RRID: AB_2109645), mouse anti-O4 (Millipore Bioscience Research Reagents, MAB345, RRID: AB_94872). After primary antibody incubation, the NSCs were rinsed 3 times with PBS and incubated in the corresponding fluorescent-conjugated secondary antibody (Table 2). Finally, cultures were counterstained with DAPI (Vector Laboratories Inc.) to label the nuclei.

2.5 | Gas chromatography analysis of fatty acid profiles

Lipid extraction from integrated mouse brain tissues and appropriate cultured adult NSCs was performed according to the general technique reported previously (Lai et al., 2006). An Agilent 7890A (Agilent Technologies, Santa Clara, CA) did the gas chromatography. Fatty acid components were identified by comparison of retention times with those of authentic standards (Sigma-Aldrich, St. Louis, MO, USA). The ratio of n-3 to n-6 was calculated by the areas of peaks.

2.6 | Adult NSCs hypoxic damage induced by $CoCl_2$

$CoCl_2$ (Sigma-Aldrich, St. Louis, MO, USA), a chemical hypoxia-mimetic agent (Cheng et al., 2017; Naves, Jawhari, Jauberteau, Ratinaud, & Verdier, 2013), was dissolved in sterile deionized water to prepare 50 mM stock solution. Different terminal concentrations (0, 50, 100, 200, 300, 400 μM) were added to $NSCs^{WT}$ to develop the adult NSC hypoxia model in vitro (Tan et al., 2009). The $NSCs^{WT}$ were seeded

into 96-well plates at a density of 5×10^4 cells per well and were treated with $CoCl_2$ at different terminal concentrations for 24 hr (Cheng et al., 2017; Lan et al., 2012; Stenger, Naves, Verdier, & Ratinaud, 2011). After the $CoCl_2$ treatment, cell viability was detected using the CellTiter-Glo Luminescent Cell Viability Assay (Promega, Madison, WI, USA) according to the manufacturer's instructions. Briefly, Cell Titer-Glo regent equal to the volume of the cell culture medium was added to each well, and the culture was then incubated at room temperature for 10 min to stabilize the luminescence signal. The luminescence signal was recorded using a multimode microplate reader (BioTek, Synergy 2, CA). The outcomes were expressed as relative cell viability (%), and half the maximal inhibitory concentration of $CoCl_2$ was designated as the optimal condition to simulate adult NSC ischemia/hypoxia (Liu et al., 2014; Tan et al., 2009).

2.7 | Adult NSCs viability assay

Dissociated $NSCs^{fat\text{-}1}$ and $NSCs^{WT}$ were precultured in opaque-walled 96-well plates at a density of 5×10^4 cells with 100 μl of SFM per well in quintuplicate, followed by hypoxic injury induced by $CoCl_2$ treatment. Then cell viability was investigated using the CellTiter-Glo Luminescent Cell Viability Assay (Promega, Madison, WI, USA) according to the manufacturer's instructions. The luminescent signal value was measured with a multimode microplate reader (BioTek, Synergy 2, CA, USA).

2.8 | Adult NSCs caspase-3 activity assay

Caspase-3 activity was detected using a caspase-3 colorimetric assay kit (BIOBOX, China) according to the manufacturer's instructions. Ac-DEVD-pNA was used as the substrate in this assay. Briefly, the Ac-DEVD-pNA complex was dissociated by active caspase-3, releasing fluorogenic pNA; thus, the fluorogenic pNA reflected the activity of caspase-3. After incubation with $CoCl_2$, cells were collected and lysed in lysis buffer on ice for 30 min. The protein concentrations of the supernatant fluids were detected with the BCA protein assay kit (Thermo Fisher Scientific, Waltham, MA, USA), and 200 μg of protein was mixed with the reaction mixture, followed by 4-hr incubation at 37 °C. The absorbance value was measured at an excitation wavelength of 405 nm and emission wavelength of 505 nm with a microplate reader (BioTek, EON, CA, USA). Caspase-3 activity was expressed as a percentage relative to controls.

2.9 | Adult NSCs proliferation index by 5-bromodeoxyuridine labeling

Proliferation of cells was evaluated by 5-bromodeoxyuridine (BrdU) incorporation assay. Dissociated adult NSCs were planted at a density of 1×10^5 cells per milliliter into 24-well plates with coverslips, which were coated with Poly-D-Lysine (Sigma-Aldrich, St. Louis, MO, USA) and sterile laminin (Roche, Mannheim, Germany). After 4 hr, experimental groups were treated with $CoCl_2$ at 200 μM terminal concentrations for 22 hr and then incubated with 10 μmol/l BrdU (Sigma-Aldrich, St. Louis, MO, USA) for 2 hr in each group. Immunocytochemical assay was used to determine the incorporation. The cultured cells were fixed in 4% paraformaldehyde for 15 min and treated with 2 M HCl for 20 min at room temperature; 0.1 M sodium borate (pH 8.5) was then added for 2 min. Blocked unspecific binding with 5% normal goat serum was performed for 30 min, followed by incubation with anti-BrdU monoclonal antibody (Abcam, ab2284, RRID: AB_302944) at room temperature for 2 hr; donkey anti-sheep IgG Alexa Fluor 594 (Invitrogen, A21099, RRID: AB_141474) was used as the secondary antibody. Nuclear DNA was labeled in blue with DAPI. The percentage of $BrdU^+$ cells was ascertained by randomly counting eight nonoverlapping microscopy fields of three coverslips for each condition; the average count was 120 cells per field. Independent experiments were done in triplicate.

2.10 | Measurement of reactive oxygen species formation

Intracellular reactive oxygen species (ROS) levels were detected by ROS fluorescent probe–dihydroethidium (DHE) assay according to the manufacturer's instructions. Briefly, the adult NSCs of each group were incubated with 1 μM DHE (Vigorous Biotechnology, Beijing, China) in the dark for 30 min. Fluorescence was measured with a Nikon ECLIPSE 80i fluorescence microscope and quantified using Image-Pro Plus analysis software (http://www.mediacy.com; RRID: SCR_007369).

2.11 | Determination of reduced GSH generation

The intracellular GSH level assay was performed using a reduced GSH assay kit (Njjcbio, China). Briefly, third-passage adult NSCs were seeded into 6-well plates at a density of 1×10^5 cells per milliliter with five replicates in each group and subjected to the various treatments described previously. Subsequently, adult NSCs were collected and lysed on ice for 30 min. The protein concentrations of the supernatant fluids were determined using the BCA protein assay kit (Thermo Fisher Scientific, Waltham, MA, USA). Intracellular GSH was then detected according to the protocol described by the manufacturer. Absorbance at 405 nm was measured with a microplate reader (BioTek, EON, CA, USA). The experiment was repeated independently 5 times.

2.12 | Quantitative real-time PCR

Total RNA was extracted from cultured adult NSCs of each group using Qiagen RNeasy Mini Kit (Qiagen, Germany). RNA samples were reverse transcribed to cDNA using Hiscript II Q RT SuperMix (Vazyme, Beijing, China). *Nrf2*, *HO-1*, *NQO-1*, and *GCLC* mRNA expression were quantified by real-time PCR (RT-PCR) with specific primers (Table 1). Samples consisted of 1 μl of cDNA per well of each reaction plate using an SYBR Green master mixture (Vazyme, Beijing, China) and normalized to β-actin. The LightCycler96 RT-PCR system (Roche, Mannheim, Germany) was used for quantitative RT-PCR analysis.

2.13 | Western blot analysis

Adult NSCs were washed twice with precooled PBS and lysed using a Nuclear and Cytoplasmic Protein Extraction Kit (BIOBOX, Nanjing, China)

TABLE 1 PCR primers used in this study

Gene	Forward (5′→3′)	Reverse (5′→3′)
Nrf2	TTCTTTCAGCAGCATCCTCTCCAC	ACAGCCTTCAATAGTCCCGTCCAG
HO-1	CAAGCCGAGAATGCTGAGTTCATG	GCAAGGGATGATTTCCTGCCAG
NQO-1	GCGAGAAGAGCCCTGATTGTACTG	TCTCAAACCAGCCTTTCAGAATGG
GCLC	ACATCTACCACGCAGTCAAGGACC	CTCAAGAACATCGCCTCCATTCAG
β-Actin	TCGTGCGTGACATTAAGGAGAAG	GTTGAAGGTAGTTTCGTGGATGC

Note: GCLC = glutamate cysteine ligase catalytic subunit; *HO-1* = heme-oxygenase-1; *NQO-1* = NADPH quinone dehydrogenase 1; *Nrf2* = nuclear factor erythroid 2-related factor 2.

according to manufacturer's instructions. Protein concentration was determined by BCA protein assay kit (Thermo Scientific), and Western blot was performed using the standard SDS-PAGE method. Primary antibodies included anti-Nrf2 (Abcam, ab2284, RRID: AB_302944), anti-*HO-1* (Abcam, ab68477, RRID: AB_11156457), anti-*NQO-1* (Abcam, ab28947, RRID: AB_881738), and anti-*GCLC* (Abcam, ab80841, RRID: AB_2107804) antibody. Histone H3 (Abcam, ab9050, RRID: AB_306966) and GAPDH (Proteintech, HRP-60004, RRID: AB_2107436) used as internal reference were detected in the nuclear fraction and cytosolic fraction, respectively. The membranes were washed for three 10-min times in TBST buffer and incubated for 1 hr at room temperature with HRP-labeled appropriate secondary antibody (Table 2). Immunoreactive proteins were visualized with the Super Signal West Femto Maximum Sensitivity Substrate (Thermo Fisher Scientific, Waltham, MA, USA). Band intensities were analyzed using Image J 1.25 software (http://rsb.info.nih.gov/ij/index.html; RRID: SCR_003070).

2.14 | Antibody characterization

All antibodies used in this study are listed in Table 2.

Mouse Anti-Rat Nestin, Clone Rat 401 (BD, 556309, RRID: AB_1645170). Nestin is an intermediate filament protein that is abundantly expressed in neuroepithelial stem cells early in embryogenesis, but is absent from nearly all mature central nervous system cells. Staining pattern was identical to that reported in publications using the same antibodies (Frederiksen & Mckay, 1988).

Anti-O4, Clone 81 (Millipore, MAB345, RRID: AB_94872). O-antigens are sulfatides, which function as differentiation markers on the surface of oligodendrocytes of the central nervous system. O4 is formed postnatally and is a marker for cell bodies and processes of oligodendrocytes types I and II. The anti-O4 antibody has been routinely evaluated by immunocytochemistry, as demonstrated previously by others using the same antibody (Li et al., 2011; Schachner et al., 1981).

Anti-GFAP, Lot 2558352 (Millipore, AB5804, RRID: AB_2109645). GFAP is the main constituent of intermediate filaments in astrocytes and serves as a cell-specific marker that distinguishes differentiated astrocytes from other glial cells during the development of the central nervous system. The staining pattern of cells and brain tissues was identical to those described in publications using the same antibodies (Benarroch et al., 2007).

Anti-Beta III Tubulin, Lot 2676286 (Millipore, AB9354, RRID: AB_570918). According to technical information from Millipore, class III beta-tubulin is a microtubule element expressed exclusively in neurons, and it is a popular marker specific for neurons in tissue. Specificity of the antibody was assessed by the manufacturer. The antibody against beta III tubulin has been used by others to visualize immature neurons of mice (Guo et al., 2011).

Anti-BrdU (Abcam, RRID: AB_302944). The immunocytochemical detection of BrdU incorporated into DNA is a powerful tool to study the cytokinetics of normal and neoplastic cells. This antibody was routinely tested by immunohistochemical analysis and demonstrated population-specific staining (Gratzner, 1982).

Anti-Nrf2 Clone EP1808Y (Abcam, ab62352, RRID: AB_944418). Transcription activator that binds to ARE elements in the promoter regions of target genes. Important for the coordinated upregulation of genes in response to oxidative stress. The antibody was evaluated by Western blotting, and results were as expected from previous descriptions (Turpaev & Drapier, 2009).

Anti-NQO1 Clone A180 (Abcam, ab28947, RRID: AB_881738). NQO1 belongs to the NAD(P)H dehydrogenase (quinone) family and is located in the cytoplasm. The Western blot of NQO1 in neural cells was consistent with that reported by others (Siegel et al., 1998).

Anti-HO-1 Clone EPR1390Y (Abcam, ab68477, RRID: AB_11156457). According to technical information from Abcam, this antibody recognizes mouse, human, and rat HO-1, which is suitable for Western blot and immunohistochemistry. HO-1 exhibits cytoprotective effects since an excess of free heme sensitizes cells to undergo apoptosis. Our Western blot results were consistent with those from other published articles using the same antibody (He et al., 2014; Maruyama et al., 2014).

Anti-GCLC (Abcam, ab80841, RRID: AB_2107804). This antibody recognizes the heavy subunit of GCLC. The GCLC antibody detected only the expected protein (73kD) on Western blot of mouse brain. The results of Western blot with GCLC were as expected from foregoing descriptions.

TABLE 2 Primary antibodies used

Antigen	Description of immunogen	Source, host species, catalog no., clone or lot no., RRID	Concentration used
Nestin	Rat(E15) spinal cord extracts	BD mouse IgG1, Cat.# 556309, Clone Rat 401, RRID: AB_1645170	1:500
O4	Homogenate of white matter ofcorpus callosum from bovine brain	Millipore mouse monoclonal, Cat.# MAB345, RRID: AB_94872	1:25
GFAP	Purified bovine GFAP	Millipore rabbit polyclonal, Cat.# AB5804, RRID: AB_2109645	1:500
Beta III tubulin	Synthetic peptide from human/ratbeta III tubulin	Millipore chicken polyclonal, Cat.# AB9354, RRID: AB_570918	1:500
NeuN	Synthetic peptide within Human NeuN aa 1-100 (Cysteine residue).	Abcam rabbit monoclonal, Cat.# ab177487, RRID: AB_2532109	1:500
BrdU	Bromodeoxyuridine coupled tokeyhole limpet hemocyanin (KLH)	Abcam sheep polyclonal, Cat.# ab2284, RRID: AB_302944	1:500
Nurf2	Synthetic peptide within human Nrf2 aa 550 to the C-terminus	Abcam rabbit monoclonal, Cat.# ab62352, RRID: AB_944418	1:1,000
HO-1	Synthetic peptide within Human Heme Oxygenase 1aa 1–100 (N terminal)	Abcam rabbit monoclonal, Cat.# ab68477, RRID: AB_11156457	1:1,000
NQO1	Recombinant full-length proteinof human NQO1	Abcam mouse polyclonal, Cat.# ab28947, RRID: AB_881738	1:1,000
GCLC	Synthetic peptide correspondingto Rat GCLC aa 295–313	Abcam rabbit polyclonal, Cat.# ab80841, RRID: AB_2107804	1:1,000
Histone H3	Synthetic peptide within humanhistone H3 aa 1-100 conjugated tokeyhole limpet haemocyanin	Abcam rabbit polyclonal, Cat.# ab9050, RRID: AB_306966	1:1,000
GAPDH	Recombinant protein	Proteintech mouse IgG2b Cat.# HRP-60004, RRID: AB_2107436	1:5,000
Rabbit IgG		SANTA CRUZ goat anti-rabbit IgGsecondary antibody, HRP conjugate Cat.# sc-2004, RRID: AB_631746	1:5,000
Mouse IgG		SANTA CRUZ goat anti-mouse IgGsecondary antibody, HRP conjugate, Cat.# sc-2005, RRID: AB_631736	1:5,000
Mouse IgG		Invitrogen goat anti-mouse IgG secondary antibody, Alexa Fluor 488 conjugate, Cat.# A21121, RRID: AB_141514	1:300
Mouse IgG(H+L)		Abcam goat anti-mouse IgG(H+L) secondary antibody, Alexa Fluor 594 conjugate, Cat.# ab307-21, RRID: AB_10897916	1:300
Sheep IgG		Invitrogen donkey anti-sheep IgG secondary antibody, Alexa Fluor 594 conjugate, Cat.# A21099, RRID: AB_141474	1:300
Rabbit IgG(H+L)		Abcam goat anti-rabbit IgG(H+L)secondary antibody, FITC conjugate, Cat.# ab6718, RRID: AB_955551	1:1,000
Rabbit IgG(H+L)		Abcam goat anti-rabbit IgG(H+L) secondary antibody, Alexa Fluor 594 conjugate, Cat.# ab96901, RRID: AB_10679699	1:500
Chicken IgY(H+L)		Thermo Fisher scientific goatanti-chicken IgY(H+L) secondaryantibody, Alexa Fluor 594 conjugate, Cat.# SA5-10072, RRID: AB_2556652	1:500

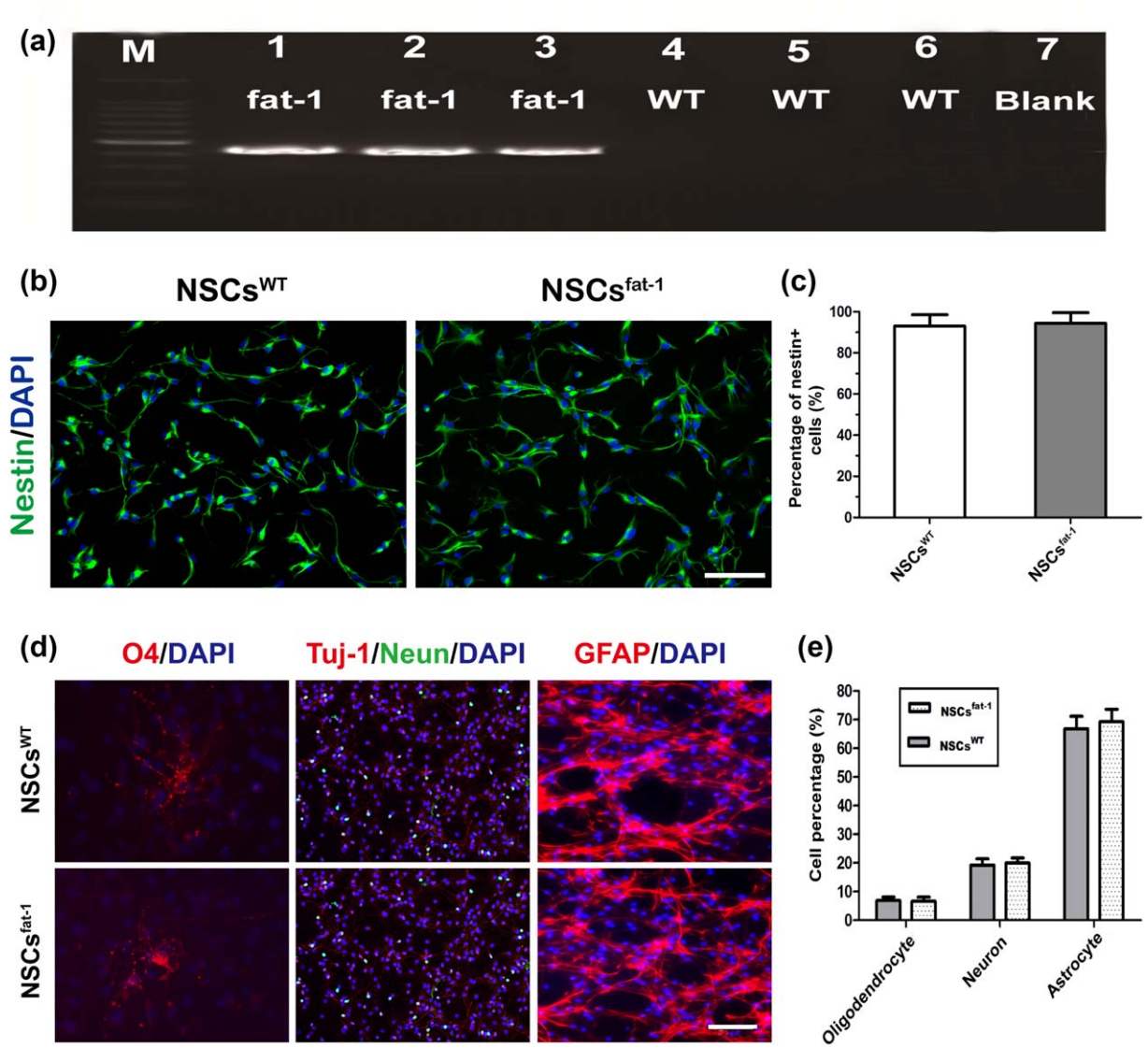

FIGURE 1 Identification of NSCs$^{fat\text{-}1}$ and NSCs^{WT}. (A) The PCR products were analyzed by agarose gel electrophoresis, which showed positive fat-1 samples (lane 1, 2, 3) and WT controls (lane 4, 5, 6). The length of positive PCR product was 438 bp. (B) Adult NSCs were identified by nestin immunostaining and counterstaining with DAPI. (C) Quantification of nestin-positive cells from the image in panel A. The nestin-positive cells in NSCs$^{fat\text{-}1}$ and NSCs^{WT} were 96% ± 2.05% and 94% ± 2.35%, respectively. Data are shown as mean ± *SD* (n = 5). (D) NeuN/Tuj1^{+} neurons, GFAP^{+} astrocytes, and O4^{+} oligodendrocytes successfully differentiated from adult NSCs. (E) Percentage of neural cells differentiated from adult NSCs was calculated based on at least four randomly selected areas of the images. Data are shown as mean ± *SD* (n = 5). The scale bars are 100 μm.

2.15 | Statistical analysis

Comparisons between two groups were subject to a two-tailed Student test. The differences between means of multiple groups were assessed by ANOVA followed by the Bonferroni/Dunn post hoc test. Statistical analysis was performed in SPSS 23 statistical software (RRID: SCR_002865; IBM, Armonk, NY). All data were presented as the mean ± *SD* of at least three independent experiments, and statistical significance was defined as $p < .05$.

3 | RESULTS

3.1 | Identification of NSCs$^{fat\text{-}1}$ and NSCs^{WT} in vitro

Tail samples were taken from adult mfat-1 transgenic mice and WT littermates. The genotypes of fat-1 transgenic mice and WT littermates were identified by PCR amplification. The PCR analysis showed high expression of the fat-1 gene in mfat-1 transgenic mice (lanes 1, 2, and 3) and negative expression in WT mice (lanes 4, 5, and 6) (Figure 1A). NSCs are capable of self-renewal and have a proliferative and multipotent capacity through

TABLE 3 Analysis of n-6 and n-3 PUFA composition

	n-6 PUFAs species, %			n-3 PUFAs Species, %					
	LA	AA	Total n-6	ALA	EPA	DPA	DHA	Total n-3	n-3/n-6 ratio
NSCsWT	0	4.03 ± 0.00	4.038 ± 0.00	0	0	0.73 ± 0.04	0.72 ± 0.07	1.45 ± 0.09	0.36 ± 0.01
NSCsfat-1	0	2.83 ± 0.00*	2.83 ± 0.00*	0	0.65 ± 0.00*	1.25 ± 0.00*	1.74 ± 0.02*	3.64 ± 0.03*	1.28 ± 0.06*
WT brain	17.24 ± 0.30	7.52 ± 0.20	24.76 ± 0.23	1.59 ± 0.04	0	0	15.00 ± 0.17	16.59 ± 0.25	0.67 ± 0.01
Fat-1 brain	15.23 ± 0.38#	6.53 ± 0.36#	21.76 ± 0.23	1.65 ± 0.04	0.06 ± 0.00#	0.16 ± 0.00#	14.28 ± 0.22	16.15 ± 0.26	0.74 ± 0.02#

Note: The cultured third-passage NSCs and whole mouse brains were collected from fat-1 transgenic mice and WT control littermates. Compositions of n-3 or n-6 PUFAs were expressed using relative percentages—that is, the distribution areas of n-3 or n-6 PUFA peaks divided by the total peak areas of all detectable saturated and unsaturated free fatty acids (from the same sample) resolved from the gas chromatography column. Data are mean ± *SD*; $n = 3$. *$p < .001$ compared with NSCs^{WT}. #$p < .001$ compared with WT mouse brain. AA = arachidonic acid; ALA = α-lipoic acid; DPA = docosapentaenoic acid; DHA = docosahexaenoic acid; EPA = eicosapentaenoic acid; LA = linoleic acid.

which they can differentiate into neurons, astrocytes, and oligodendrocytes. Nestin, an intermediate filament protein, is specifically expressed in NSCs. NSCs$^{fat\text{-}1}$ and NSCs^{WT} from certified adult mice were cultured into adherent monolayers to examine their "stem" and "differentiation" abilities. The nestin immunostaining showed that there was no significant difference in positive cells between NSCs$^{fat\text{-}1}$ and NSCs^{WT} ($p > .05$; Figure 1B,C). Furthermore, the differentiating experiment showed that NSCs$^{fat\text{-}1}$ and NSCs^{WT} both succeeded in differentiating into Tuj1^{+} neurons, GFAP^{+} astrocytes, and O4^{+} oligodendrocytes, with no statistical difference (Figure 1D,E).

3.2 | Expression of the *mfat-1* transgene elevated the n-3/n-6 PUFA ratio

Fatty acid analyses of mfat-1 transgenic mice and WT littermates were performed using GC-MS. The whole mouse brains and cultured third-passage NSCs were detected. As shown in Table 3, NSCs$^{fat\text{-}1}$ exhibited a decreased proportion of n-6 PUFAs, including AA, and increased expression of n-3 PUFAs, including EPA, DPA, and DHA, which resulted in sharp elevation of n-3/n-6 ratio relative to those in the NSCs^{WT} (1.28 ± 0.06 in NSCs$^{fat\text{-}1}$ vs. 0.36 ± 0.02 in NSCs^{WT}; Student *t* test, $n = 3$, *$p < .001$). Compared with NSCs, the ratio of n-3/n-6 in the mouse brain was modestly increased (0.74 ± 0.02 in fat-1 brain vs. 0.67 ± 0.01 in WT brain; Student *t* test, $n = 3$, #$p < .001$).

3.3 | NSC$^{fat\text{-}1}$ activity was enhanced against $CoCl_2$-induced hypoxic injury

Cultured cells exposed to $CoCl_2$ for 24 hr are widely used to establish a hypoxic injury model (Li et al., 2013; Tan et al., 2009; Zhang, Qian, Pan, Li, & Zhu, 2012). To identify the optimal $CoCl_2$ concentration, NSCs^{WT} were treated with different $CoCl_2$ concentrations (0, 50, 100, 200, 300, and 400 μM) for 24 hr, and cell viability was measured by the CellTiter-Glo Luminescent Cell Viability Assay (Promega). As shown in Figure 2A, NSC viability was robustly reduced in a dose-dependent manner. Exposure to 200 μM $CoCl_2$ for 24 hr resulted in a cell viability loss of about 50%, which was identified as the optimal experimental condition for an adult NSC hypoxic injury model in vitro (Liu et al., 2014).

We then investigated the protective effects of the high ratio of n-3/n-6 PUFA on NSCs$^{fat\text{-}1}$ that were treated with the adult NSC hypoxic injury model. After 200 μM $CoCl_2$ exposure for 24 hr, as shown in Figure 2B, the cell viability rate of NSCs$^{fat\text{-}1}$ + $CoCl_2$(24h) was significantly increased compared with NSCs^{WT} + $CoCl_2$(24h) (68.2% ± 5.9% in NSCs$^{fat\text{-}1}$ + $CoCl_2$ vs. 49.3% ± 3.1% in NSCs^{WT} + $CoCl_2$; Student *t* test, $n = 3$, *$p < .001$). The results indicate that NSCs$^{fat\text{-}1}$ were protected against $CoCl_2$-induced hypoxic injury.

3.4 | *mfat-1* transgene inhibited $CoCl_2$-mediated NSCs$^{fat\text{-}1}$ apoptosis

After 200 μmol/l $CoCl_2$ treatment for 24 hr, we detected the caspase-3 activity of each group. Only a small amount of intrinsic apoptosis was detected in cultured NSCs$^{fat\text{-}1}$ and NSCs^{WT} without $CoCl_2$ treatment, and caspase-3 activity was almost the same between the two groups

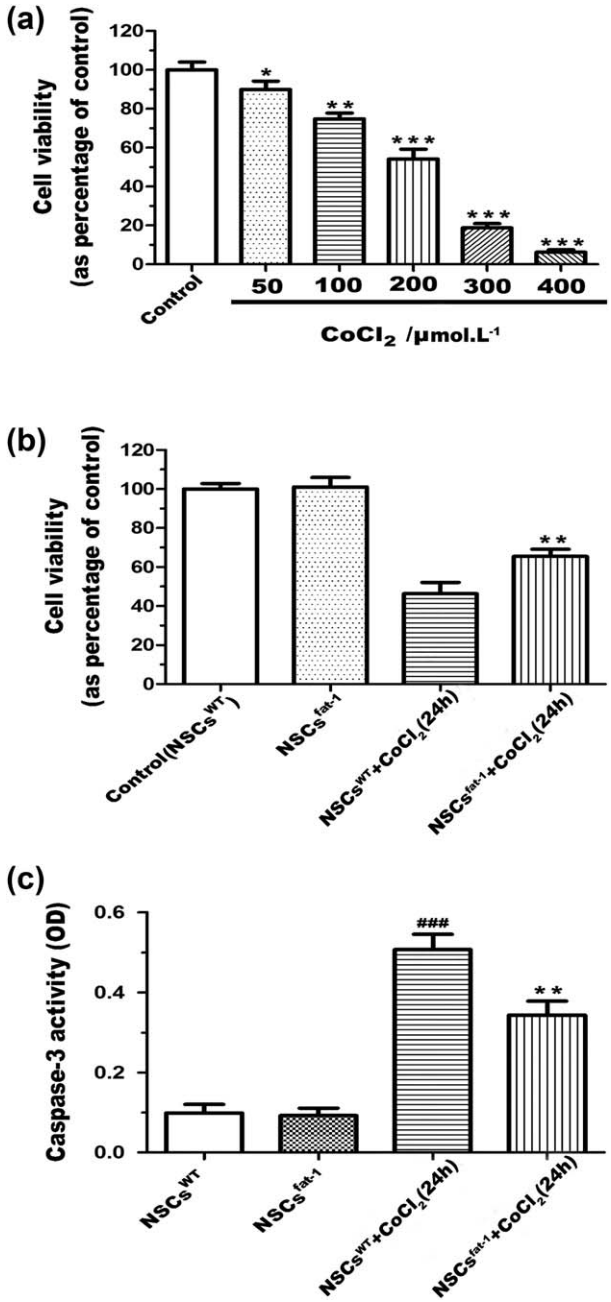

FIGURE 2 $NSCs^{fat\text{-}1}$ increased cell activity against $CoCl_2$-mediated apoptosis. (A) Establishment of adult NSC hypoxic injury model in vitro. Cell viability assays showed that exposure to $CoCl_2$ for 24 hr caused dramatic NSC hypoxia damage in a dose-dependent manner. $CoCl_2$ exposure at a concentration of 200 μmol/l for 24 hr caused approximately 50% cell loss. Data represent the mean ± *SD*, $n = 5$ per group. $^{*}p < .05$, $^{**}p < .01$, and $^{***}p < .001$ vs. control. (B) Cell viability of adult NSCs was evaluated after 200 μmol/l $CoCl_2$ exposure for 24 hr by CellTiter-Glo Luminescent Cell Viability Assay. $CoCl_2$-induced cell death was prevented in $NSCs^{fat\text{-}1}$. Values are expressed as mean ± *SD* of three independently repeated experiments. $^{**}p < .01$ vs. $NSCs^{WT} + CoCl_2$. (C) $NSCs^{fat\text{-}1}$ inhibited $CoCl_2$-induced increase in caspase-3 activity. The NSC apoptosis rate of each group was measured by detecting caspase-3 activity. In the $CoCl_2$-treated groups, caspase-3 activity was significantly decreased in the $NSCs^{fat\text{-}1} + CoCl_2$(24h) group compared with the $NSCs^{WT} + CoCl_2$(24h) group. Values represent five replicates of values in three independent experiments (mean ± *SD*). $^{**}p < .01$ vs. $NSCs^{WT} + CoCl_2$. $^{\#\#\#}p < .001$ vs. $NSCs^{WT}$.

($p > .05$; Figure 2C). In contrast, $NSCs^{fat\text{-}1} + CoCl_2$(24h) showed a significant decrease in caspase-3 activity (32.7% ± 2.9%) compared with $NSCs^{WT} + CoCl_2$(24h) (51.4% ± 3.1%) ($^{**}p < .01$; Figure 2C). $NSCs^{fat\text{-}1}$ exhibited anti–hypoxic injury properties. These findings indicate that a high n-3/n-6 PUFA ratio could protect NSCs against $CoCl_2$-mediated hypoxic injury.

3.5 | *mfat-1* transgene promoted proliferation of adult NSCs against $CoCl_2$-mediated injury

To further investigate the anti–hypoxic damage effects of a high n-3/n-6 PUFA ratio in adult NSCs, we used the BrdU labeling assay to quantify the adult NSC proliferation rate. BrdU staining showed no

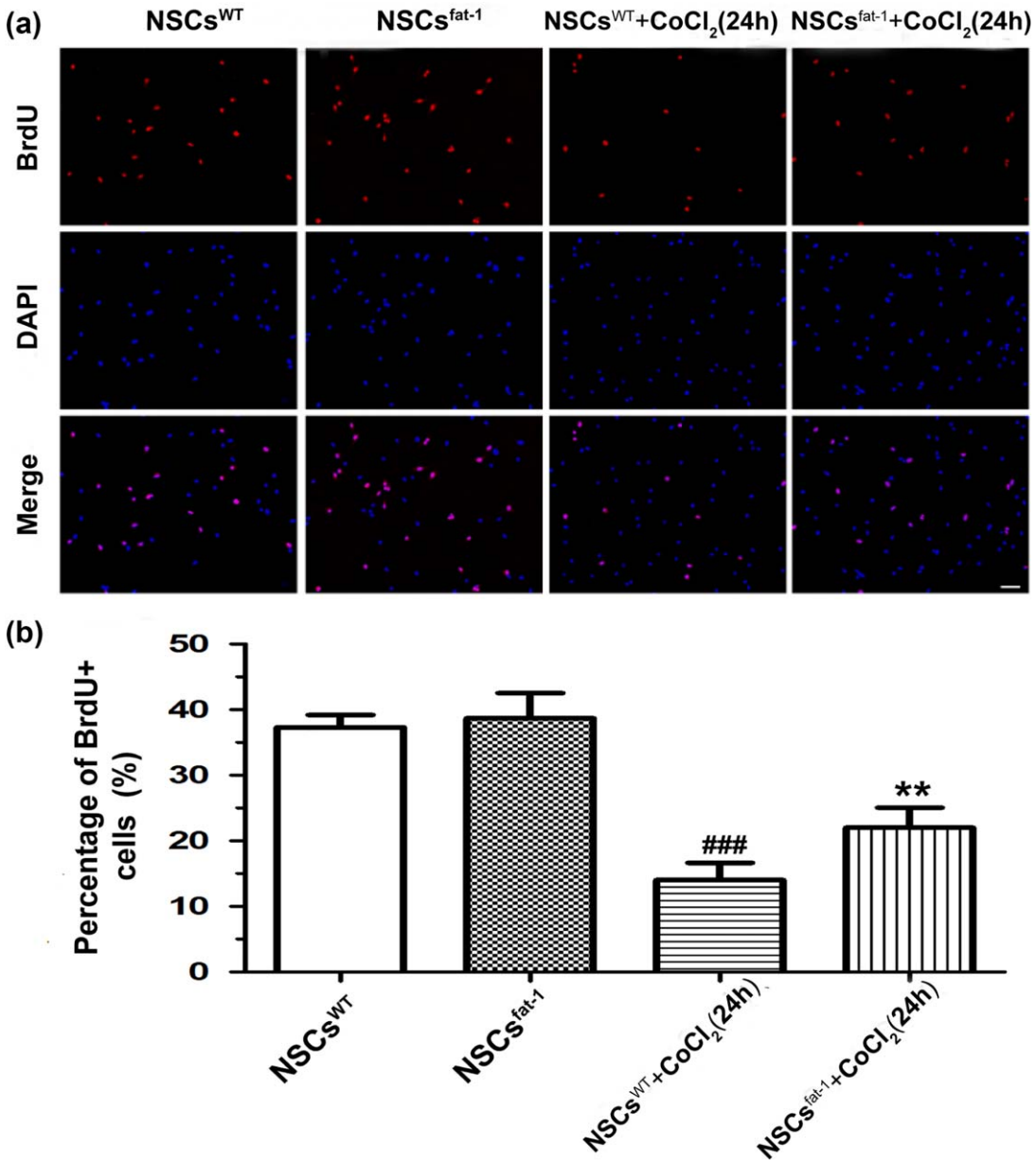

FIGURE 3 mfat-1 transgene effectively inhibited $CoCl_2$-induced reduction of adult NSC proliferation. (A) After incubation with $CoCl_2$ or vehicle, cells were subjected to bromodeoxyuridine (BrdU) assay (red), counterstained with DAPI (blue), and photographed with fluorescent microscopy. The mfat-1 transgene increased the bromodeoxyuridine labeling of adult NSCs in the $NSCs^{fat\text{-}1}$ + $CoCl_2$(24h) group compared with the $NSCs^{WT}$ + $CoCl_2$(24h) group. (B) Quantification of $BrdU^+$ adult NSCs over all $DAPI^+$ cells. Bar graphs were selected as representative data from five independent experiments. Data represent mean ± *SD* of five independent experiments. $^{**}p < .01$ vs. $NSCs^{WT}$ + $CoCl_2$(24h) group. $^{\#\#\#}P < .001$ vs. NSC^{WT}. Scale bar = 100 μm.

significant difference between the $NSC^{fat\text{-}1}$ and NSC^{WT} groups before $CoCl_2$-mediated hypoxic injury (37.6% ± 1.8% in $NSCs^{fat\text{-}1}$ vs. 38.2% ± 3.1% in $NSCs^{WT}$; Student *t* test, $n = 5$, $p > .05$; Figure 3A,B). Around 24.58% ± 2.61% of cells were found to be $BrdU^+$ in the $NSCs^{fat\text{-}1}$ + $CoCl_2$(24h) group, while the rate of BrdU positivity was significantly decreased in the $NSCs^{WT}$ + $CoCl_2$(24h) group, in which only 17.13% ± 2.44% of cells were found to be $BrdU^+$ ($^{**}p < .01$; Figure 3A,B). The results suggest that a high n-3/n-6 PUFA ratio protected cultured adult NSCs from $CoCl_2$-mediated hypoxic injury and promoted the proliferation of adult NSCs against $CoCl_2$-induced hypoxic injury.

3.6 | *mfat-1* transgene improved $CoCl_2$-mediated adult NSCS injury through antioxidative damage

It has been reported that oxidative stress–induced adult NSC apoptosis plays a critical role in the pathogenesis of ischemic stroke and its complications (Chehaibi et al., 2016; Yamauchi et al., 2016). Oxidative stress is a primary factor that has been shown to affect adult NSC function, differentiation, and survival (Wang, Liu, et al., 2014). To determine whether the protective role of the mfat-1 transgene on adult NSCs in hypoxic-ischemic damage might relate to oxidative stress, we

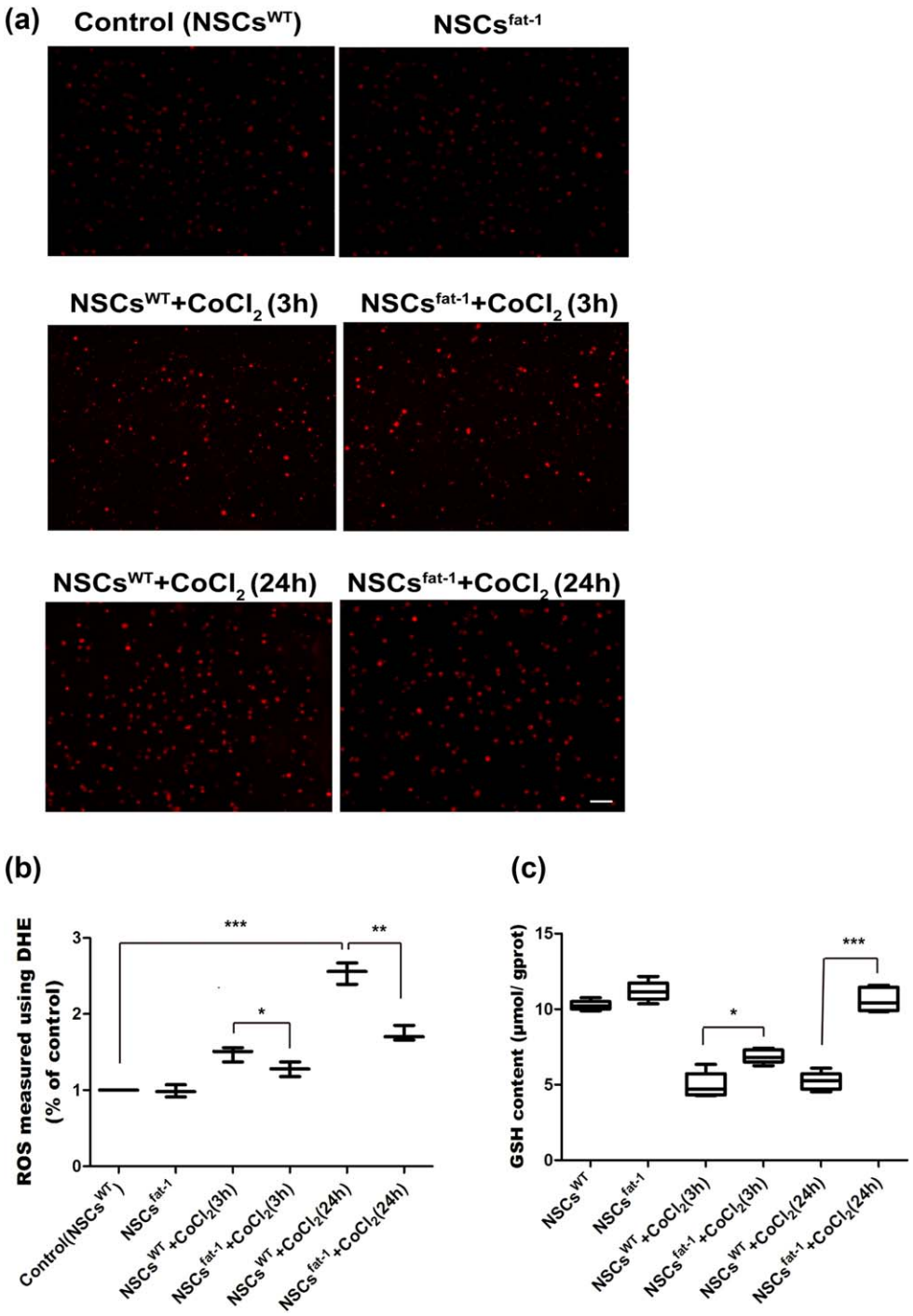

FIGURE 4 Reduced ROS expression and increased generation of GSH were demonstrated in $NSCs^{fat\text{-}1}$ after $CoCl_2$-mediated hypoxic injury. (A) Representative DHE-stained images of adult NSCs showing ROS generation in each group. ROS production in $NSC^{fat\text{-}1}$ + $CoCl_2$(24h) was considerably attenuated compared with $NSCs^{WT}$ + $CoCl_2$(24h). Scale bar = 100 μm. (B) Quantification of DHE fluorescence image from panel A, $^*p < .05$ vs. $NSCs^{WT}$ + $CoCl_2$(3h), $^{**}p < .01$ vs. $NSCs^{WT}$ + $CoCl_2$(24h), $^{***}p < .001$ vs. control, $n = 3$. (C) Results of GSH concentration in the cultured NSCs. Data shown are mean ± *SD*. $^*p < .05$ vs. $NSCs^{WT}$ + $CoCl_2$(3h), $^{***}p < .001$ vs. $NSCs^{WT}$ + $CoCl_2$(24h), $n = 5$. Student *t* test, $p < .05$. [Color figure can be viewed at wileyonlinelibrary.com]

measured intracellular superoxide formation by DHE assay and then examined intracellular GSH levels with a reduced GSH assay kit. The DHE assay consists of fluorogenic probes designed to reliably measure ROS in live cells, whose signal is localized primarily in the nucleus. As shown in Figure 4B, when $NSCs^{fat\text{-}1}$ and $NSCs^{WT}$ were exposed to 200 μmol/l $CoCl_2$ for 3 hr, a significant difference existed between $NSCs^{fat\text{-}1}$ + $CoCl_2$(3h) and $NSCs^{WT}$ + $CoCl_2$(3h) (124% ± 7.9% vs. 148% ± 9.8%, $^*p < .05$); when $NSCs^{fat\text{-}1}$ and $NSCs^{WT}$ were exposed

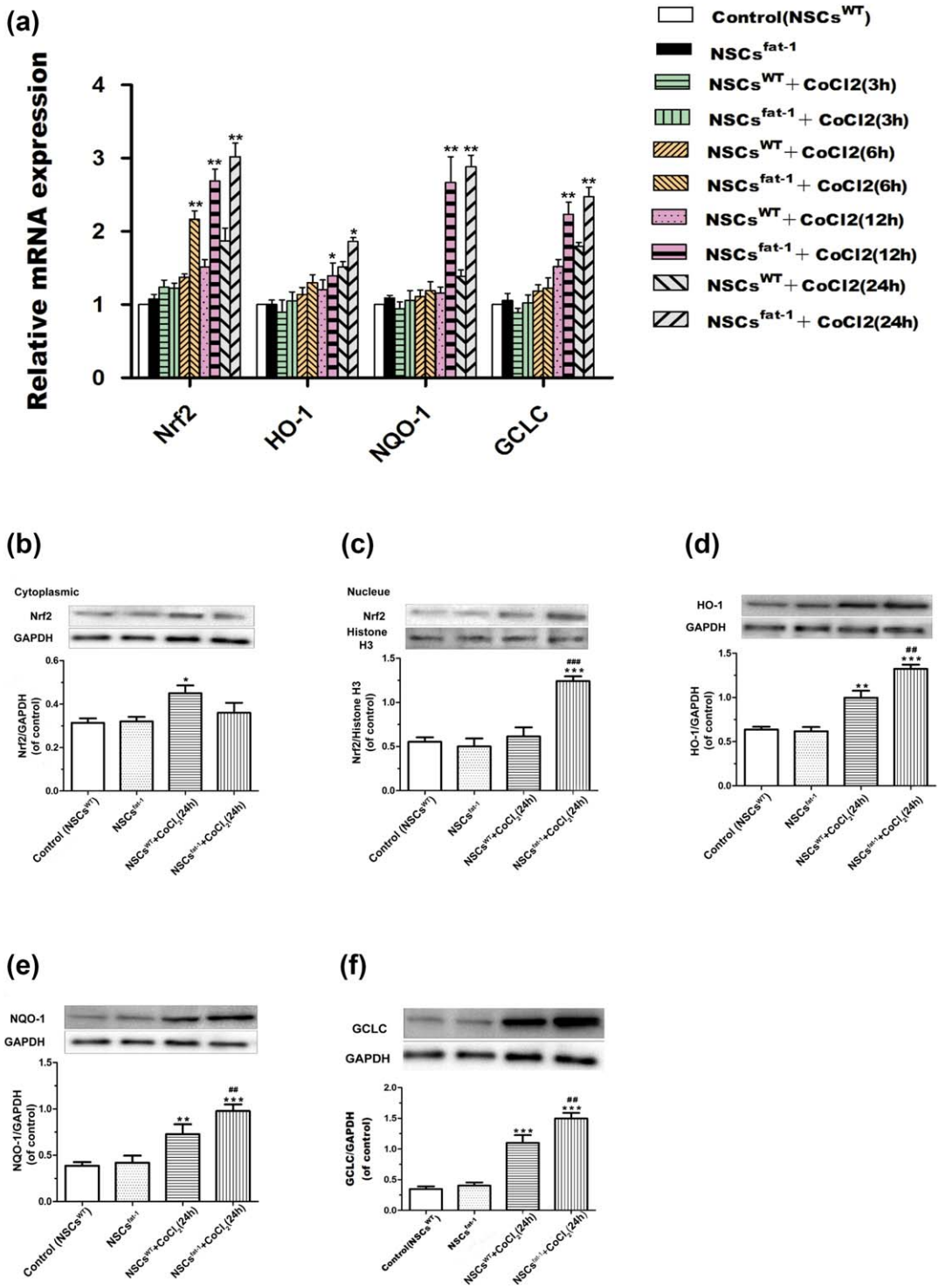

FIGURE 5 NSCs^{fat-1} upregulated the Nrf2-ARE signal pathway and increased the expression of downstream genes and phase II detoxification genes (*HO-1*, *NQO-1*, *GCLC*). (A) In $CoCl_2$-treated groups, quantitative RT-PCR indicated that NSC^{fat-1} induced significant increases in the mRNA expression level of Nrf2 and its downstream genes and phase II detoxification gene transcripts *HO-1*, *NQO-1*, and *GCLC* compared with NSCs^{WT} + $CoCl_2$. β-actin was used as an internal control. Values represent the mean ± *SD* of three independent experiments. $^{*}p < .05$, $^{**}p < .01$ vs. the same-time $CoCl_2$-treated group. NSCs^{fat-1} were treated with 200 μM $CoCl_2$ or vehicle for 24 hr, and were lysed and fractionated to isolate nuclear and cytosolic fractions as indicated. (B, C) Western blotting analysis and quantification of cytoplasmic and nuclear *Nrf2* protein. Cytoplasmic and nuclear proteins were normalized by *GAPDH* and histone *H3*, respectively ($n = 3$). (D, E, F) Western blotting analysis and quantification of *HO-1*, *NQO-1*, and *GCLC* protein expression separately ($n = 3$). Data are presented as mean ± *SD*; $^{*}p < .05$, $^{**}p < .01$, and $^{***}p < .001$ vs. control. $^{\#\#}p < .01$ and $^{\#\#\#}p < .001$ vs. NSCs^{WT} + $CoCl_2$(24h) group. [Color figure can be viewed at wileyonlinelibrary.com]

to 200 μmol/l $CoCl_2$ for 24 hr, the intracellular ROS level (mean fluorescent intensity) significantly increased (248% ± 4.54% of control, ***$p < .001$), and there was a significant difference between the two groups (173% ± 11.72% in $NSCs^{fat\text{-}1}$ + $CoCl_2$(24h) vs. 248% ± 9.54% in $NSCs^{WT}$ + $CoCl_2$(24h), **$p < .01$), revealing that $NSCs^{WT}$ exposed to $CoCl_2$ displayed intense fluorescence after being stained with DHE probe reagent, while intracellular ROS accumulation resulting from $CoCl_2$ exposure was remarkably reduced in $NSCs^{fat\text{-}1}$ (Student *t* test, $n = 3$, *$p < .05$, **$p < .01$; Figure 4A,B).

To further explore possible mechanisms underlying the beneficial effects of a high n-3/n-6 PUFA ratio, a reduced GSH assay kit was used to evaluate the expression of GSH, a potent ROS scavenger, in cultured $NSCs^{WT}$ and $NSCs^{fat\text{-}1}$ after $CoCl_2$ insult. Production of GSH was detected at different time points in $NSCs^{fat\text{-}1}$ and $NSCs^{WT}$ after $CoCl_2$ insult. As shown in Figure 4C, a statistical difference existed between $NSCs^{WT}$ and $NSCs^{fat\text{-}1}$ after $CoCl_2$ insult for 3 hr. We also investigated the 24-hr time point. The results show that the production of GSH increased notably in $NSCs^{fat\text{-}1}$ compared with $NSCs^{WT}$ after $CoCl_2$ insult for 24 hr (10.63 ± 0.71 in $NSCs^{fat\text{-}1}$ + $CoCl_2$(24h) vs. 5.24 ± 1.18 in $NSCs^{WT}$ + $CoCl_2$(24h)); Student *t* test, $n = 5$, ***$p < .001$; Figure 4C). Collectively, oxidative stress is implicated in the pathogenesis of $CoCl_2$-mediated hypoxic injury in vitro, and a high n-3/n-6 PUFA ratio exhibits a protective effect on adult NSCs by increasing GSH levels and enhancing the capacity of scavenging ROS.

3.7 | Nrf2-ARE signal pathway is involved in protective effects of $NSCs^{fat\text{-}1}$

Several recent studies have shown Nrf2 to be a critical transcription factor that regulates a battery of antioxidant genes in the response to oxidative stress (Ma, 2013). Therefore, to study the antioxidative mechanisms, we first investigated whether Nrf2, the principal transcription factor that regulates the basal and inducible expression of a battery of antioxidant genes, was upregulated. Quantitative RT-PCR analysis showed that in the 24-hr $CoCl_2$-treated groups, $NSCs^{fat\text{-}1}$ induced a nearly 2.3-fold increase in the mRNA transcript level of Nrf2 compared with $NSCs^{WT}$ (**$p < .01$; Figure 5A). Furthermore, prominent increases in the expression level of the downstream gene and phase II detoxification gene (*HO-1*, *NQO-1*, *GCLC*) were found in $NSCs^{fat\text{-}1}$ + $CoCl_2$(24h) compared with $NSCs^{WT}$ + $CoCl_2$(24h) (Figure 5A). To further elucidate the mechanisms of activation of Nrf2/ARE pathways, the temporal sequence of the *Nrf2* signal was investigated. The expression level of the relevant genes (*Nrf2*, *HO-1*, *NQO-1*, *GCLC*) was detected by quantitative RT-PCR at different time points. As shown in Figure 5A, an increase in the expression level of the Nrf2 gene preceded antioxidant enzyme genes, and antioxidant enzyme gene transcripts (*HO-1*, *NQO-1*, *GCLC*) began to increase at the 6-hr time point, which indicated that the nuclear translocation of *Nrf2* occurs before the expressions of antioxidant enzymes.

As nuclear translocation of the protein *Nrf2* is very important in inducing the expression of antioxidant genes, the protein levels of cytosolic and nuclear fraction *Nrf2* were observed by Western blot. Consistent with quantitative RT-PCR results, Western blot analysis showed that in the 24-hr $CoCl_2$-treated groups, $NSCs^{fat\text{-}1}$ robustly increased the protein expression of nuclear *Nrf2* compared with $NSCs^{WT}$ (Figure 5B), while the expression level of cytosolic *Nrf2* in $NSCs^{fat\text{-}1}$ was significantly decreased compared with $NSCs^{WT}$ (Figure 5C). In addition, the expression of *Nrf2*-related antioxidant defense enzymes such as *HO-1*, *NQO-1*, and *GCLC* was substantially increased (Figure 5D–F). These results indicate that the mfat-1 transgene promoted the nuclear translocation of *Nrf2* and upregulated endogenous antioxidants through an *Nrf2*-dependent signaling pathway in $CoCl_2$-mediated adult NSC hypoxic injury.

4 | DISCUSSION

The cell injury induced by hypoxia is a primary concern in various clinical fields, such as ischemic stroke and NSC transplantation (Chen, Zhang, Gu, & Guo, 2016). $CoCl_2$-induced cell hypoxic damage in NSCs can serve as a simple and convenient in vitro model (Chen et al., 2009; Sandner et al., 1997; Tan et al., 2009; Zou et al., 2001), which provides a chance to investigate the effect of a high n-3/n-6 PUFA ratio on adult NSCs against hypoxic-ischemic damage in vitro and to elucidate the underlying molecular mechanisms.

Decades of research have shown that a high n-3/n-6 PUFA ratio could protect the neural system against hypoxic-ischemic damage. Hu et al. (2013) reported that n-3 PUFA supplementation is a potential neurogenic and oligodendrogenic treatment to naturally improve poststroke brain repair and long-term functional recovery. Using a mouse model of transient focal cerebral ischemia, researchers concluded that n-3 fatty acids could potentially play a role in poststroke cerebrovascular remodeling (Wang, Shi, et al., 2014). The n-3 PUFAs exerted protective effects on neurons against ischemic injury both in vitro and in vivo, partly through inhibiting ROS activation (Shi et al., 2016). However, little information is available on the role of n-3 PUFAs in protecting adult NSCs from hypoxic injury after $CoCl_2$-induced hypoxic damage at a cellular level.

In the present study, we first investigated the effects of $CoCl_2$ on adult NSCs and successfully established an adult NSC hypoxic injury model in vitro. To explore the protective effects of the high ratio of n-3/n-6 PUFAs on adult $NSCs^{fat\text{-}1}$ subjected to the adult NSC hypoxic injury model, the cell viability and cell apoptosis were investigated by CellTiter-Glo Luminescent Cell Viability Assay (Promega) and caspase-3 colorimetric assay (BIOBOX, China), respectively. The results show that a high n-3/n-6 PUFA ratio could exert protective effects against $CoCl_2$-induced cell viability loss and also decreased the apoptotic rate throughout the experiment. Next, an experiment was performed to detect the proliferation index of adult NSCs against $CoCl_2$-mediated injury, which showed that the rate of BrdU positivity was significantly increased in the $NSCs^{fat\text{-}1}$ + $CoCl_2$(24h) group compared with the $NSCs^{WT}$ + $CoCl_2$(24h) group. Collectively, the results indicate that mfat-1 transgenic adult NSCs with a high n-3/n-6 PUFA ratio were protected from hypoxic damage induced by $CoCl_2$.

The mechanisms underlying the protective effect of the *mfat-1* transgene against hypoxic damage to adult NSCs from $CoCl_2$ are still

not fully understood. Previous studies have reported that oxidative stress–induced neuronal apoptosis plays an important role in the pathogenesis of ischemic stroke (Chehaibi et al., 2016; Yamauchi et al., 2016). Recent investigations have indicated that overproduction of n-3 PUFAs is highly effective in protecting the brain, and that there are protective mechanisms involved in *Nrf2* activation and *HO-1* upregulation (Zhang et al., 2014). One study also found that n-3 PUFAs enhanced the phosphorylation of Akt after ischemic stroke by regulating phosphatidylserine (Akbar, Calderon, Wen, & Kim, 2005). However, these factors may not clarify the adult NSCs' protective mechanism. In the present study, we demonstrated that oxidative stress is implicated in the pathogenesis of $CoCl_2$-mediated hypoxic injury in vitro, and that a high n-3/n-6 PUFA ratio exerts a protective effect on NSCs by increasing GSH levels and enhancing the capacity of scavenging ROS. Subsequently, we investigated the *Nrf2/ARE* signal pathway, a key pathway of antioxidative stress. *Nrf2* is a transcription factor that plays a key role in cytoprotection against oxidative stress (Dou et al., 2016; Ma, 2013). Under basal conditions *Nrf2* is mostly retained in the cellular cytosol by binding of its *Neh2* domain to *Keap1*, which in turn is anchored to actin cytoskeleton (Kobayashi et al., 2004). *Keap1* is a cysteine-rich cytosolic protein that functions as an adaptor, leading to the proteasomal degeneration of *Nrf2* via ubiquitination. Under stressful conditions, the *Nrf2–Keap-1* complex is dissociated and *Nrf2* rapidly undergoes nuclear translocation, initiating the expression of antioxidative and detoxifying enzymes (Dou et al., 2016). The activated *Nrf2* upregulates the transcription of numerous antioxidant and phase II detoxification genes to provide protective effects in many neurological diseases (Nanou et al., 2013; Zhang et al., 2014). Our quantitative RT-PCR analysis showed that a much higher expression of *Nrf2* and its downstream genes (*HO-1*, *NQO-1*, *GCLC*) was found in the $NSCs^{fat\text{-}1} + CoCl_2$(24h) group than in the $NSCs^{WT} + CoCl_2$(24h) group. Subsequently, Western blot results showed that a high n-3/n-6 PUFAs ratio enhanced *Nrf2* translocation from the cytoplasm to the nucleus of cultured adult NSCs after $CoCl_2$ treatment for 24 hr and substantially increased the expression of *Nrf2*-related antioxidant defense enzymes such as *HO-1*, *NQO-1*, and *GCLC*. In summary, our results reveal that a high n-3/n-6 PUFA ratio has a neuroprotective effect on adult NSCs against $CoCl_2$-mediated hypoxic injury, and the underlying molecular mechanism may involve the activation of the *Nrf2/ARE* pathway. Although our study has revealed the neuroprotective mechanism of *mfat-1*, the potential antioxidant effects of *mfat-1* have yet to be established clearly, but they may be important. The *fat-1* gene can convert n-6 to n-3 PUFAs, leading to a higher n-3/n-6 PUFA ratio. Fluidity of plasma membrane plays important roles for cellular functions such as signal transduction, cell recognition, membrane order and the funtion of membrane receptors; flexibility of plasma membrane could increase membrane stability, which can adapt to challenge of different conditions (Lafourcade et al., 2011; Yamashima, 2008). The ratio of n-3/n-6 has a positive correlation with membrane fluidity and flexibility, which can be involved in antioxidative effects and upregulate the expression of antioxidant enzyme genes in $NSCs^{Fat\text{-}1}$ to enhance the capacity of scavenging ROS (Hasadsri et al., 2013; Lee et al., 2014; Ying, Feng, Agrawal, Zhuang, & Gomez-Pinilla, 2012).

In recent years, NSC replacement therapy has emerged as a promising potential treatment for ischemic stroke (Kokaia & Darsalia, 2011). Because of their many advantages (Giusto et al., 2014), adult NSCs have been regarded as an excellent source of replacement therapy for human ischemic stroke. However, the primary obstacle to clinical application is the loss of physiological function of endogenous NSCs and exogenous adult NSCs resulting from hypoxic-ischemic injury in the ischemic penumbra (Azevedo-Pereira & Daadi, 2013; Bazan et al., 2005; Rosenblum et al., 2015). Our results provide valuable information for the development of effective adult NSC replacement therapy for ischemic stroke. With regard to endogenous adult NSC replacement therapy, the n-3/n-6 PUFA ratio can be increased by dietary or other means, resulting in increased protection of adult NSCs from hypoxic-ischemic damage to get better support for self-repair of neural function damage. For exogenous adult NSC replacement therapy, the n-3/n-6 PUFA ratio of adult NSCs could be elevated with an engineered gene for *mfat-1*. A combination of the above two therapies could achieve optimal restoration of neurological function in ischemic stroke.

ACKNOWLEDGMENTS

The authors thank their colleagues in the Jiangsu Key Laboratory of Xenotransplantation, Nanjing.

CONFLICT OF INTEREST

The authors declare no competing financial interests.

AUTHOR CONTRIBUTIONS

All authors had full access to all the data in the study and take responsibility for the integrity of the data and the accuracy of the data analysis. Study concept and design: Y.W., J.F.Y. Acquisition of data: J.F.Y., Y.W., B.F. Analysis and interpretation of data: J.F.Y., Y. W., H.Y.Y. Drafting of the manuscript: J.F.Y., Y.W. Critical revision of the article for important intellectual content: Y.W., H.Y.Y. Statistical analysis: J.F.Y., H.Y.Y. Obtained funding: Y.F.D. Technical and material support: J.F.Y., Y.W. Study supervision: Y.W.

REFERENCES

Akbar, M., Calderon, F., Wen, Z., & Kim, H. Y. (2005). Docosahexaenoic acid: A positive modulator of Akt signaling in neuronal survival. *Proceedings of the National Academy of Sciences of the United States of America*, *102*, 10858–10863.

Antonny, B., Vanni, S., Shindou, H., & Ferreira, T. (2015). From zero to six double bonds: Phospholipid unsaturation and organelle function. *Trends in Cell Biology*, *25*, 427–436.

Arvidsson, A., Collin, T., Kirik, D., Kokaia, Z., & Lindvall, O. (2002). Neuronal replacement from endogenous precursors in the adult brain after stroke. *Nature Medicine*, *8*, 963–970.

Azevedo-Pereira, R. L., & Daadi, M. M. (2013). Isolation and purification of self-renewable human neural stem cells for cell therapy in experimental model of ischemic stroke. *Methods in Molecular Biology*, *1059*, 157–167.

Bazan, N. G., Marcheselli, V. L., & Cole-Edwards, K. (2005). Brain response to injury and neurodegeneration: Endogenous

neuroprotective signaling. *Annals of the New York Academy of Sciences*, *1053*, 137–147.

Benarroch, E. (2007). Endocannabinoids in basal ganglia circuits: implications for Parkinson disease. *Neurology*, *69*, 306–309.

Belayev, L., Khoutorova, L., Atkins, K. D., & Bazan, N. G. (2009). Robust docosahexaenoic acid-mediated neuroprotection in a rat model of transient, focal cerebral ischemia. *Stroke*, *40*, 3121–3126.

Belayev, L., Khoutorova, L., Atkins, K. D., Eady, T. N., Hong, S., Lu, Y., ... Bazan, N. G. (2011). Docosahexaenoic acid therapy of experimental ischemic stroke. *Translational Stroke Research*, *2*, 33–41.

Chang, Y. L., Chen, S. J., Kao, C. L., Hung, S. C., Ding, D. C., Yu, C. C., ... Chiou, S. H. (2012). Docosahexaenoic acid promotes dopaminergic differentiation in induced pluripotent stem cells and inhibits teratoma formation in rats with Parkinson-like pathology. *Cell Transplantation*, *21*, 313–332.

Chehaibi, K., Trabelsi, I., Mahdouani, K., & Slimane, M. N. (2016). Correlation of oxidative stress parameters and inflammatory markers in ischemic stroke patients. *Journal of Stroke and Cerebrovascular Diseases*, *25*, 2585–2593.

Chen, J. X., Zhao, T., & Huang, D. X. (2009). Protective effects of edaravone against cobalt chloride-induced apoptosis in PC12 cells. *Neuroscience Bulletin*, *25*, 67–74.

Chen, L., Zhang, G., Gu, Y., & Guo, X. (2016). Meta-analysis and systematic review of neural stem cells therapy for experimental ischemia stroke in preclinical studies. *Scientific Reports*, *6*, 32291.

Cheng, B. C., Chen, J. T., Yang, S. T., Chio, C. C., Liu, S. H., & Chen, R. M. (2017). Cobalt chloride treatment induces autophagic apoptosis in human glioma cells via a p53-dependent pathway. *International Journal of Oncology*, *50*, 964–974.

Chung, T. N., Kim, J. H., Choi, B. Y., Chung, S. P., Kwon, S. W., & Suh, S. W. (2015). Adipose-derived mesenchymal stem cells reduce neuronal death after transient global cerebral ischemia through prevention of blood-brain barrier disruption and endothelial damage. *Stem Cells Translational Medicine*, *4*, 178–185.

Cramer, S. C. (2008). Repairing the human brain after stroke. II. Restorative therapies. *Annals of Neurology*, *63*, 549–560.

Dinkova-Kostova, A. T., & Talalay, P. (2008). Direct and indirect antioxidant properties of inducers of cytoprotective proteins. *Molecular Nutrition & Food Research*, *52*(Suppl. 1), S128–S138.

Dou, T., Yan, M., Wang, X., Lu, W., Zhao, L., Lou, D., ... Zhou, Z. (2016). Nrf2/ARE pathway involved in oxidative stress induced by paraquat in human neural progenitor cells. *Oxidative Medicine and Cellular Longevity*, *2016*, 8923860.

Frederiksen, K., & McKay, R. D. (1988). Proliferation and differentiation of rat neuroepithelial precursor cells in vivo. *The Journal of neuroscience*, *8*, 1144–1151.

Giusto, E., Donega, M., Cossetti, C., & Pluchino, S. (2014). Neuro-immune interactions of neural stem cell transplants: From animal disease models to human trials. *Experimental Neurology*, *260*, 19–32.

Gratzner, H. G. (1982). Monoclonal antibody to 5-bromo- and 5-iododeoxyuridine: A new reagent for detection of DNA replication. *Science*, *218*, 474–475.

Guichardant, M., Chantegrel, B., Deshayes, C., Doutheau, A., Moliere, P., & Lagarde, M. (2004). Specific markers of lipid peroxidation issued from n-3 and n-6 fatty acids. *Biochemical Society Transactions*, *32*(Pt. 1), 139–140.

Guo, J., Qiang, M., & Luduena, R. F. (2011). The distribution of beta-tubulin isotypes in cultured neurons from embryonic, newborn, and adult mouse brains. *Brain research*, *1420*, 8–18.

Hasadsri, L., Wang, B. H., Lee, J. V., Erdman, J. W., Llano, D. A., Barbey, A. K., ... Wang, H. (2013). Omega-3 fatty acids as a putative treatment for traumatic brain injury. *Journal of Neurotrauma*, *30*, 897–906.

Hong, S. H., Belayev, L., Khoutorova, L., Obenaus, A., & Bazan, N. G. (2014). Docosahexaenoic acid confers enduring neuroprotection in experimental stroke. *Journal of the Neurological Sciences*, *338*, 135–141.

Hu, X., Zhang, F., Leak, R. K., Zhang, W., Iwai, M., Stetler, R. A., ... Chen, J. (2013). Transgenic overproduction of omega-3 polyunsaturated fatty acids provides neuroprotection and enhances endogenous neurogenesis after stroke. *Current Molecular Medicine*, *13*, 1465–1473.

He, M., Pan, H., Chang, R. C., So, K. F., Brecha, N. C., & Pu, M. (2014), Activation of the Nrf2/HO-1 antioxidant pathway contributes to the protective effects of Lycium barbarum polysaccharides in the rodent retina after ischemia-reperfusion-induced damage. *PloS one*, *9*, e84800.

Kobayashi, A., Kang, M. I., Okawa, H., Ohtsuji, M., Zenke, Y., Chiba, T., ... Yamamoto, M. (2004). Oxidative stress sensor Keap1 functions as an adaptor for Cul3-based E3 ligase to regulate proteasomal degradation of Nrf2. *Molecular and Cellular Biology*, *24*, 7130–7139.

Koch, P., Kokaia, Z., Lindvall, O., & Brustle, O. (2009). Emerging concepts in neural stem cell research: Autologous repair and cell-based disease modelling. *Lancet Neurology*, *8*, 819–829.

Kokaia, Z., & Darsalia, V. (2011). Neural stem cell-based therapy for ischemic stroke. *Translational Stroke Research*, *2*, 272–278.

Lafourcade, M., Larrieu, T., Mato, S., Duffaud, A., Sepers, M., Matias, I., ... Manzoni, O. J. (2011). Nutritional omega-3 deficiency abolishes endocannabinoid-mediated neuronal functions. *Nature Neuroscience*, *14*, 345–350.

Lai, L., Kang, J. X., Li, R., Wang, J., Witt, W. T., Yong, H. Y., ... Dai, Y. (2006). Generation of cloned transgenic pigs rich in omega-3 fatty acids. *Nature Biotechnology*, *24*, 435–436.

Lan, A. P., Xiao, L. C., Yang, Z. L., Yang, C. T., Wang, X. Y., Chen, P. X., ... Feng, J. Q. (2012). Interaction between ROS and p38MAPK contributes to chemical hypoxia-induced injuries in PC12 cells. *Molecular Medicine Reports*, *5*, 250–255.

Lee, E. J., Yun, U. J., Koo, K. H., Sung, J. Y., Shim, J., Ye, S. K., ... Kim, Y. N. (2014). Down-regulation of lipid raft-associated onco-proteins via cholesterol-dependent lipid raft internalization in docosahexaenoic acid-induced apoptosis. *Biochimica et Biophysica Acta*, *1841*, 190–203.

Li, K. R., Zhang, Z. Q., Yao, J., Zhao, Y. X., Duan, J., Cao, C., & Jiang, Q. (2013). Ginsenoside Rg-1 protects retinal pigment epithelium (RPE) cells from cobalt chloride (CoCl2) and hypoxia assaults. *PloS One*, *8*, e84171.

Liu, M., Zhou, L., Zhang, B., He, M., Dong, X., Lin, X., ... Zheng, H. (2016). Elevation of n-3/n-6 PUFAs ratio suppresses mTORC1 and prevents colorectal carcinogenesis associated with APC mutation. *Oncotarget*, *7*, 76944–76954.

Liu, Q., Wu, D., Ni, N., Ren, H., Luo, C., He, C., ... Su, H. (2014). Omega-3 polyunsaturated fatty acids protect neural progenitor cells against oxidative injury. *Marine Drugs*, *12*, 2341–2356.

Ma, Q. (2013). Role of nrf2 in oxidative stress and toxicity. *Annual Review of Pharmacology and Toxicology*, *53*, 401–426.

Maruyama, A., Mimura, J., & Itoh, K. (2014). Non-coding RNA derived from the region adjacent to the human HO-1 E2 enhancer selectively regulates HO-1 gene induction by modulating Pol II binding. *Nucleic Acids Res*, *42*, 13599–13614.

Mozaffarian, D., Benjamin, E. J., Go, A. S., Arnett, D. K., Blaha, M. J., Cushman, M., ... Turner, M. B.; American Heart Association Statistics Committee; Stroke Statistics Subcommittee. (2016). Heart disease

and stroke statistics—2016 update: A report from the American Heart Association. *Circulation*, *133*, e38–e360.

Nanou, A., Higginbottom, A., Valori, C. F., Wyles, M., Ning, K., Shaw, P., & Azzouz, M. (2013). Viral delivery of antioxidant genes as a therapeutic strategy in experimental models of amyotrophic lateral sclerosis. *Molecular Therapy*, *21*, 1486–1496.

Naves, T., Jawhari, S., Jauberteau, M. O., Ratinaud, M. H., & Verdier, M. (2013). Autophagy takes place in mutated p53 neuroblastoma cells in response to hypoxia mimetic CoCl(2). *Biochemical Pharmacology*, *85*, 1153–1161.

Paradisi, M., Alviano, F., Pirondi, S., Lanzoni, G., Fernandez, M., Lizzo, G., ... Calza, L. (2014). Human mesenchymal stem cells produce bioactive neurotrophic factors: Source, individual variability and differentiation issues. *International Journal of Immunopathology and Pharmacology*, *27*, 391–402.

Rosenblum, S., Smith, T. N., Wang, N., Chua, J. Y., Westbroek, E., Wang, K., & Guzman, R. (2015). BDNF pretreatment of human embryonic-derived neural stem cells improves cell survival and functional recovery after transplantation in hypoxic-ischemic stroke. *Cell Transplantation*, *24*, 2449–2461.

Sandner, P., Wolf, K., Bergmaier, U., Gess, B., & Kurtz, A. (1997). Hypoxia and cobalt stimulate vascular endothelial growth factor receptor gene expression in rats. *Pflugers Archiv: European Journal of Physiology*, *433*, 803–808.

Schnitzer, J., & Schachner, M. (1981). Developmental expression of cell type-specific markers in mouse cerebellar cells in vitro. *J Neuroimmunol*, *1*, 471–487.

Shi, Z., Ren, H., Luo, C., Yao, X., Li, P., He, C., ... Su, H. (2016). Enriched endogenous omega-3 polyunsaturated fatty acids protect cortical neurons from experimental ischemic injury. *Molecular Neurobiology*, *53*, 6482–6488.

Siegel, D., Franklin, W. A., & Ross, D. (1998). Immunohistochemical detection of NAD(P)H:quinone oxidoreductase in human lung and lung tumors. *Clin Cancer Res*, *4*, 2065–2070.

Sims, N. R., & Muyderman, H. (2010). Mitochondria, oxidative metabolism and cell death in stroke. *Biochimica et Biophysica Acta*, *1802*, 80–91.

Stankowski, J. N., & Gupta, R. (2011). Therapeutic targets for neuroprotection in acute ischemic stroke: Lost in translation? *Antioxidants & Redox Signaling*, *14*, 1841–1851.

Stenger, C., Naves, T., Verdier, M., & Ratinaud, M. H. (2011). The cell death response to the ROS inducer, cobalt chloride, in neuroblastoma cell lines according to p53 status. *International Journal of Oncology*, *39*, 601–609.

Sun, Y., Wang, M., Liu, H., Wang, J., He, X., Zeng, J., ... Wang, L. (2011). Development of an O-antigen serotyping scheme for Cronobacter sakazakii. *Appl Environ Microbiol*, *77*, 2209–2214.

Tan, C. B., Gao, M., Xu, W. R., Yang, X. Y., Zhu, X. M., & Du, G. H. (2009). Protective effects of salidroside on endothelial cell apoptosis induced by cobalt chloride. *Biological & Pharmaceutical Bulletin*, *32*, 1359–1363.

Turpaev, K., & Drapier, J. C. (2009). Stimulatory effect of benzylidenemalononitrile tyrphostins on expression of NO-dependent genes in U-937 monocytic cells. *European journal of pharmacology*, *606*, 1–8.

Wang, D., Curtis, A., Papp, A. C., Koletar, S. L., & Para, M. F. (2012). Polymorphism in glutamate cysteine ligase catalytic subunit (GCLC) is associated with sulfamethoxazole-induced hypersensitivity in HIV/AIDS patients. *BMC Med Genomics*, *5*, 32.

Wang, J., Shi, Y., Zhang, L., Zhang, F., Hu, X., Zhang, W., ... Chen, J. (2014). Omega-3 polyunsaturated fatty acids enhance cerebral angiogenesis and provide long-term protection after stroke. *Neurobiology of Disease*, *68*, 91–103.

Wang, Z., Liu, D., Zhang, Q., Wang, J., Zhan, J., Xian, X., ... Hao, A. (2014). Palmitic acid affects proliferation and differentiation of neural stem cells in vitro. *Journal of Neuroscience Research*, *92*, 574–586.

Wei, D., Li, J., Shen, M., Jia, W., Chen, N., Chen, T., ... Zhao, A. (2010). Cellular production of n-3 PUFAs and reduction of n-6-to-n-3 ratios in the pancreatic beta-cells and islets enhance insulin secretion and confer protection against cytokine-induced cell death. *Diabetes*, *59*, 471–478.

Yamashima, T. (2008). A putative link of PUFA., GPR40 and adult-born hippocampal neurons for memory. *Progress in Neurobiology*, *84*, 105–115.

Yamauchi, K., Nakano, Y., Imai, T., Takagi, T., Tsuruma, K., Shimazawa, M., ... Hara, H. (2016). A novel nuclear factor erythroid 2-related factor 2 (Nrf2) activator RS9 attenuates brain injury after ischemia reperfusion in mice. *Neuroscience*, *333*, 302–310.

Ying, Z., Feng, C., Agrawal, R., Zhuang, Y. M., & Gomez-Pinilla, F. (2012). Dietary omega-3 deficiency from gestation increases spinal cord vulnerability to traumatic brain injury-induced damage. *PloS One*, *7*, e52998.

Zhang, M., An, C., Gao, Y., Leak, R. K., Chen, J., & Zhang, F. (2013). Emerging roles of Nrf2 and phase II antioxidant enzymes in neuroprotection. *Progress in Neurobiology*, *100*, 30–47.

Zhang, M., Wang, S., Mao, L., Leak, R. K., Shi, Y., Zhang, W., ... Zhang, F. (2014). Omega-3 fatty acids protect the brain against ischemic injury by activating Nrf2 and upregulating heme oxygenase 1. *Journal of Neuroscience*, *34*, 1903–1915.

Zhang, Q., Qian, Z., Pan, L., Li, H., & Zhu, H. (2012). Hypoxia-inducible factor 1 mediates the anti-apoptosis of berberine in neurons during hypoxia/ischemia. *Acta Physiologica Hungarica*, *99*, 311–323.

Zhang, W., Hu, X., Yang, W., Gao, Y., & Chen, J. (2010). Omega-3 polyunsaturated fatty acid supplementation confers long-term neuroprotection against neonatal hypoxic-ischemic brain injury through anti-inflammatory actions. *Stroke*, *41*, 2341–2347.

Zou, W. G., Yan, M. D., Xu, W. J., Huo, H. R., Sun, L. Y., Zheng, Z. C., & Liu, X. Y. (2001). Cobalt chloride induces PC12 cells apoptosis through reactive oxygen species and accompanied by AP-1 activation. *Journal of Neuroscience Research*, *64*, 646–653.

How to cite this article: Yu J, Yang H, Fang B, Zhang Z, Wang Y, Dai Y. *mfat-1* transgene protects cultured adult neural stem cells against cobalt chloride–mediated hypoxic injury by activating *Nrf2/ARE* pathways. *J Neuro Res*. 2017;00:1–16. https://doi.org/10.1002/jnr.24096